

Supplimentary Information

Large-Scale Synthesis and Functionalization of Hexagonal Boron Nitride

Nanosheets

Ganesh Rahul Bhimanapati, Daniel Kozuch, Joshua A Robinson*

Department of Material Science and Engineering, The Pennsylvania State
University, University Park, Pennsylvania, 16803, USA.

*Email: jrobinson@psu.edu

Table of Contents:

S0: Characterization

S1: Atomic Force Microscopy (AFM)

S2: Fourier Transform Infrared Spectroscopy (FTIR)

S3: Raman Spectroscopy

S4: X-Ray Diffraction (XRD) data analysis

S5: X-Ray Photoelectron Spectroscopy (XPS)

S0: Details of Characterization

Surface morphology and flake size was investigated using field emission scanning electron microscopy (FESEM). High resolution transmission electron microscopy (HR-TEM) images were taken using JOEL 2010F field-emission microscope at an accelerated voltage of 200 kV using a single tilt sample holder to observe the atomic structure of the hBN. The samples for TEM were prepared by suspending a low concentration of the hBN in ethanol and dropped on the Lacey carbon grids. X-ray photoelectron spectroscopy (XPS) measurements were performed immediately after the exfoliation in order to identify the elemental composition and bonding information in hBN. This was performed using XPS Kratos Ultra with an Al K α micro-focused monochromatic source (1486.6 eV) and spot size of 400 μm at an operating pressure of 5×10^{-9} Pa. Further spectroscopic evidence of the observed functionality was confirmed by using Fourier Transform InfraRed Spectroscopy (FTIR). This was performed on Bruker IFS 66/S microscope. The samples for FTIR were prepared by mixing 0.1 mg of hBN sample with 500 mg of KBr and was made into a pellet before the spectra was collected. This reduced the absorbance of the hBN sample. Crystallinity of the exfoliated hBN and the defect correlation can be made using X-ray diffraction (XRD) and Raman spectroscopy. Raman spectra were collected using a confocal WiTec α -200 Raman microscope with a 488 nm laser source (laser power: 25mW) and an integration time of 3 seconds. X-Ray diffraction spectra were collected on Panalytical Xpert Pro MPD system with a spot size of 10 mm using a Cu K α (8027 eV). The optical absorption of hBN was made using a Perkin-Elmer Lambda 950 UV-Vis-NIR spectrophotometer. The thicknesses of the samples were measured using Bruker Icon dimension. The samples for AFM were made by drop casting a drop of hBN in water on SiO₂ substrate.

The weight balance of hBN samples was made using a micro balance in a TGA. The sample weight after exfoliation was obtained by dispersing the exfoliated hBN in IPA or ethanol and drying it on aluminum boat. Typically, for about 1 gram of starting material, we get about 230-250 mg of exfoliated hBN which is about 25% of the total weight. Depending on the temperature variations during the exfoliation process, the yield can go as low as 12%. So, it is really important to maintain the temperature closer to 75°C (reaction temperature).

S1: Atomic Force Microscopy (AFM)

The flake thicknesses of the exfoliated sheets were measured by AFM. The samples for AFM were prepared by drop casting the exfoliated hBN on Silicon wafer. This induced the flakes to stack on top of each other as it can be seen in figure S1. The two different spots that were analyzed shows that the flakes that are stacked are mono layer and bi layer materials. The thickness for these flakes were 0.413 nm and 0.837 nm, which are consistent with previously reported AFM thickness (0.4-0.5 nm for monolayer, 0.8-0.9 nm for bi layer and 1.2-1.3 nm for three layer system) of few layer hBN.¹

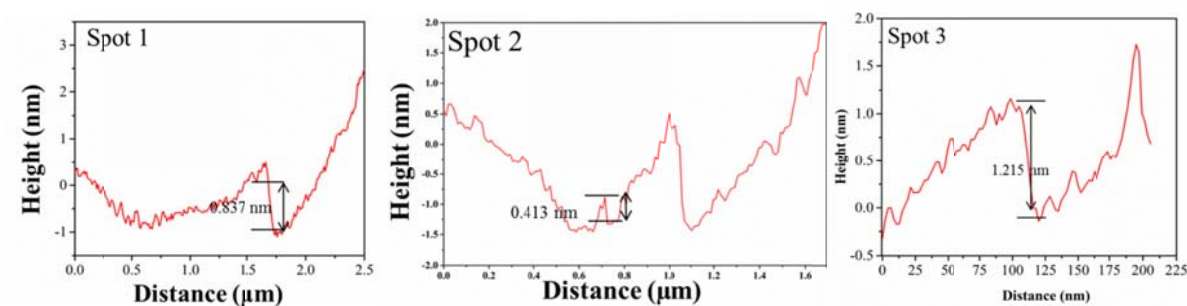
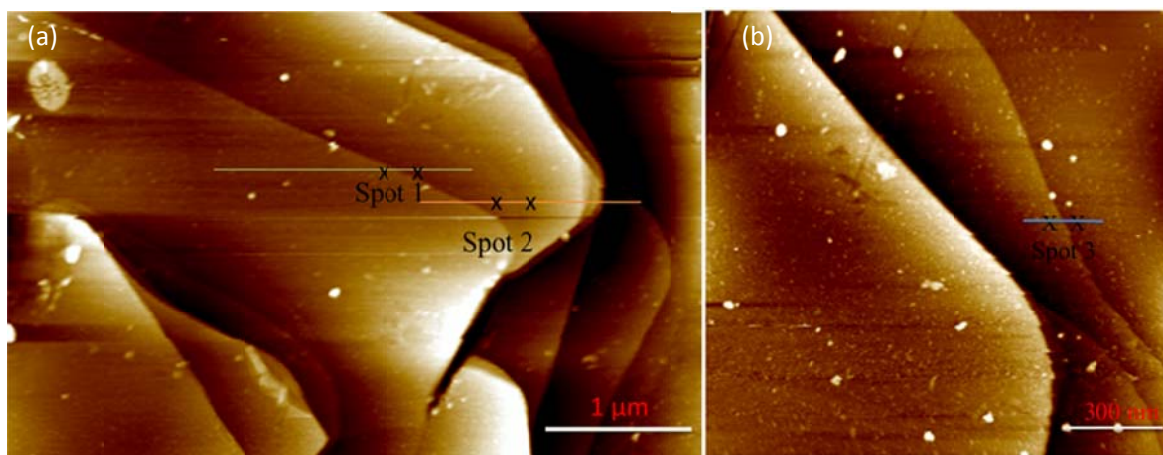


Figure S1: AFM image of exfoliated hBN and its corresponding height measurements at different spots.

S2: Fourier Transform Infra-Red Spectroscopy

FTIR was used to identify the functionality in the exfoliated hBN. As hBN is highly absorbing material, the sample had to be diluted using KBr powder (0.1 mg of hBN in 500 mg of KBr) in order to obtain an accurate spectra. The characteristic B-N stretching mode is typically observed at 1366 cm^{-1} for the exfoliated sample along with the out of plane bending mode at 814 cm^{-1} respectively. From Figure S2, we can also see that there is an addition of new peak at 1154 cm^{-1} and a significant increase in the peak at 3450 cm^{-1} which could correspond to the addition of oxygen in the sample and these peaks can be indexed to B-O vibrational mode and -OH absorption in the sample². Also, we can see that the full width half maximum for the exfoliated

peak has increased by 15 cm^{-1} which could be related to the addition of the functional groups to the structure.

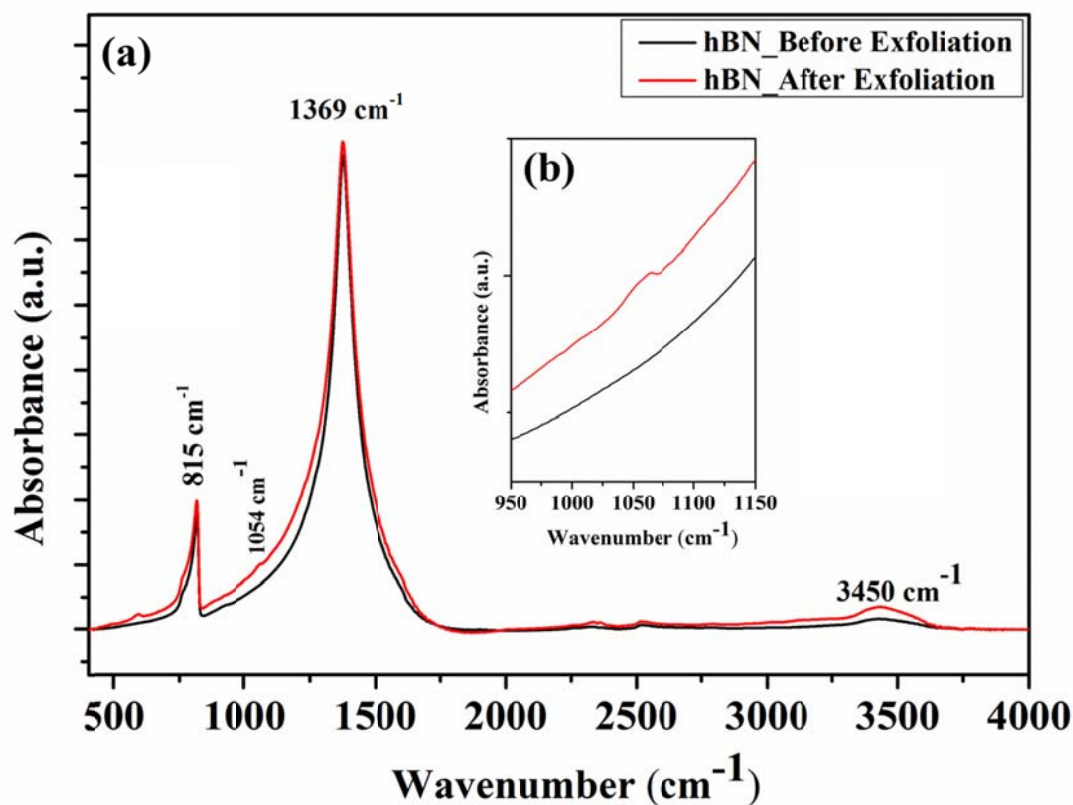


Figure S2: (a) FTIR spectra of hBN before and after exfoliation. (b) Picture showing the presence of a new peak at 1054 cm^{-1} which corresponds to B-O bonding.

S3: Raman Spectroscopy

The Raman spectra for the bulk vs exfoliated hBN is shown in **figure S3**. We can see that the peak broadens when compared with that of the bulk hBN and the intensity of the peak is reduced by 85% when compared with the bulk. This reduction in intensity is observed when the layer thickness is reduced and defects are created in the structure of the hBN. This shift in the peak position can be linked to the strain which is caused due to the stretching of the sheets and hence a red shift in the peak is observed in the Raman spectra. This observed strain-induced shift is

similar to that of graphene, where the G peak is red-shifted as much as 20 cm^{-1} . As pointed out by Watanabe *et. Al.*,¹ the strain induced shifts in pristine graphene can be covered by doping effects³ which move the G peak in graphene by $\sim 10\text{ cm}^{-1}$. As these doping effects are absent in hBN, we don't see a lot of shift ($\sim 3\text{ cm}^{-1}$) in the peak position. Also, FWHM for exfoliated hBN (22 cm^{-1}) does not change significantly when compared with the bulk hBN (20 cm^{-1}) which signifies that there is significantly less strain induced in the material during the exfoliation process.

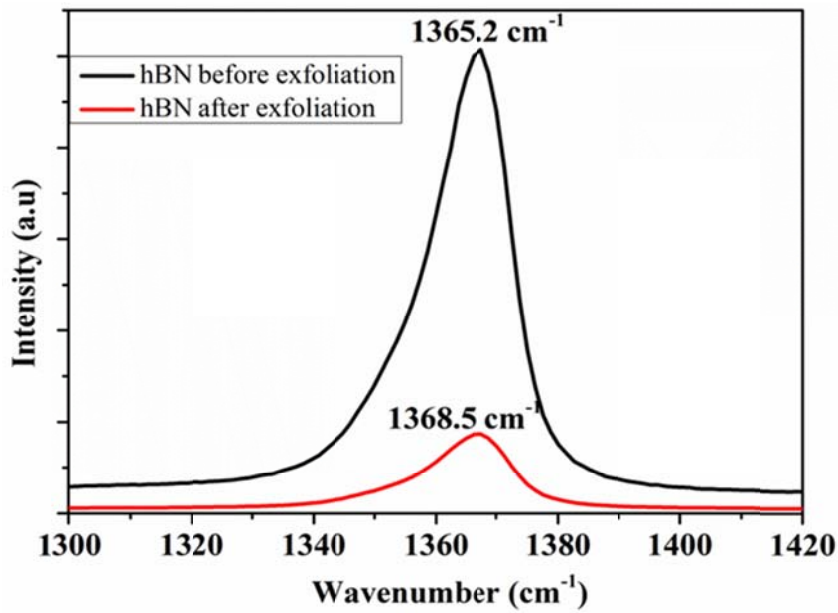


Figure S3: Raman spectra of bulk hBN Vs exfoliated hBN, showing a shift of 3.3 cm^{-1} indicating a significant reduction of sheet thickness.

S4 XRD data analysis:

From the Joint Committee on Powder Diffraction Standards (card number 34-0421) for hBN powders, the diffraction peaks can be indexed to the hBN crystals (lattice constants $a=b= 2.504$ and $c=6.656\text{ \AA}$). The observed peaks in the hBN (**Figure S4**) spectra are at $2\theta = 26.764^\circ$, 41.597° , 55.164° with a d-spacing of 3.328 \AA , 2.169 \AA and 1.663 \AA which can be correlated to the (002), (100) and (004) planes of hBN where the (004) is parallel to the (002) plane. The

intensity of the (004) plane is higher when we compare the ratio of intensities of (004) and (100) planes in bulk hBN and exfoliated hBN. I_{004}/I_{100} is 2.5 for bulk hBN and I_{004}/I_{100} is 6 for the exfoliated hBN indicating the effectiveness of the exfoliation process. As the hBN sheets tend to lie on their widest facets when they are dispersed randomly on a substrate, we found that (002) planes are the widest according to the measurement, concluding that the exfoliation occurred at the (002) plane.

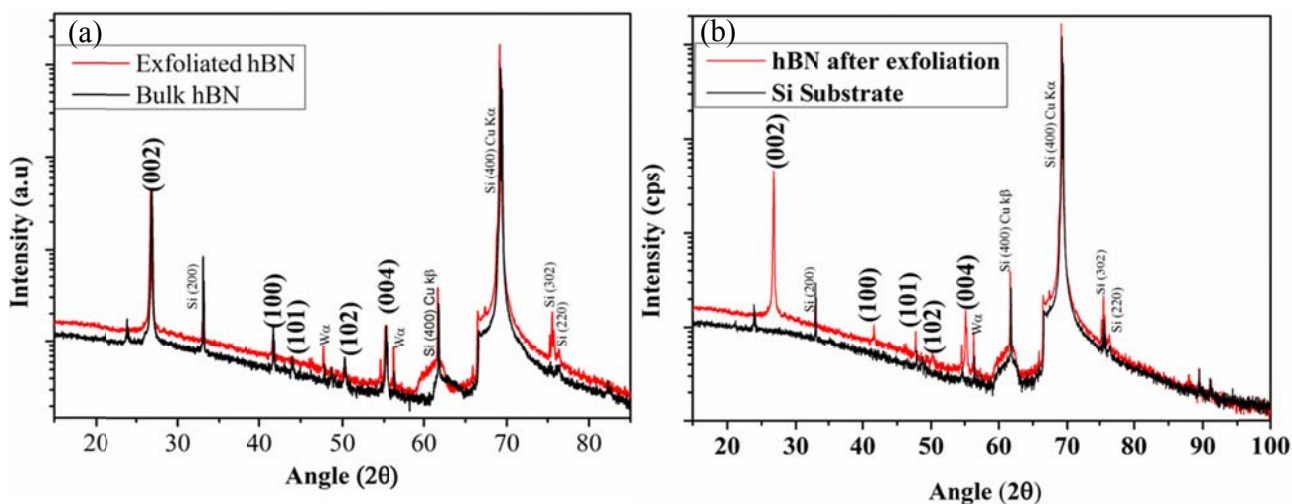


Figure S4: X-ray diffraction pattern for (a) hBN before and after exfoliation, (b) hBN and bare Si substrate.

S5 X-ray Photoelectron Spectroscopy analysis

In order to calculate the elemental percent and to deconvolute the high resolution peaks of B1s, N1s and O 1s, CASA XPS was used. The elemental composition as observed from the survey spectrum is shown in **figure S5**. By comparing the survey spectrum, we can clearly see that the % oxygen in the hBN after exfoliation has increased when compared to the hBN before exfoliation.

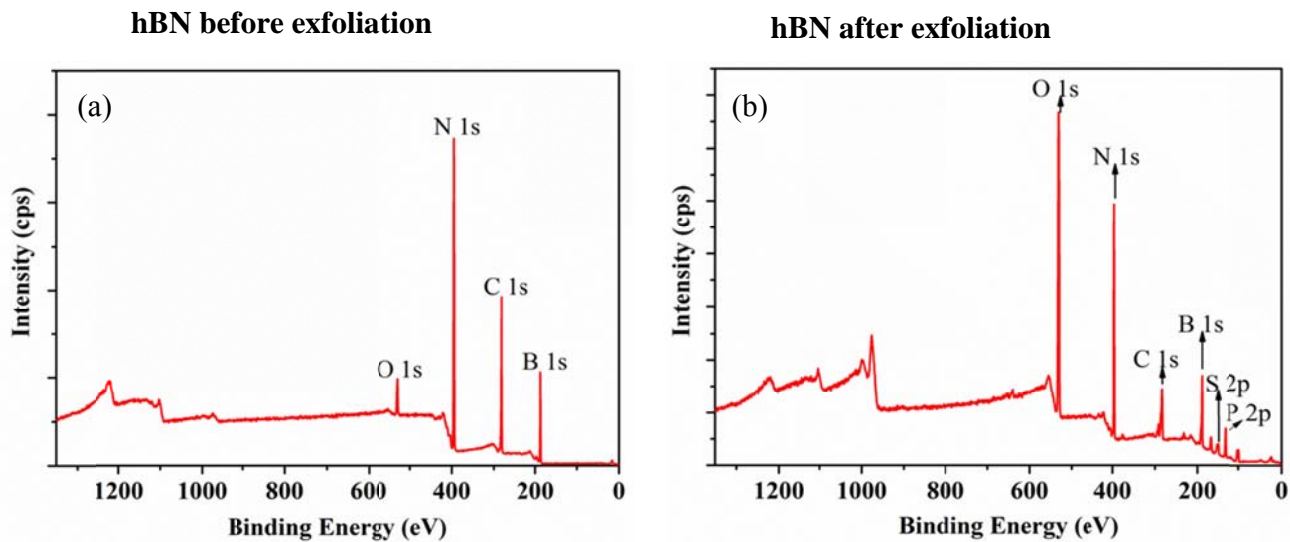


Figure S5: Plot showing the survey spectrum for hBN (a) before exfoliation and (b) after exfoliation.

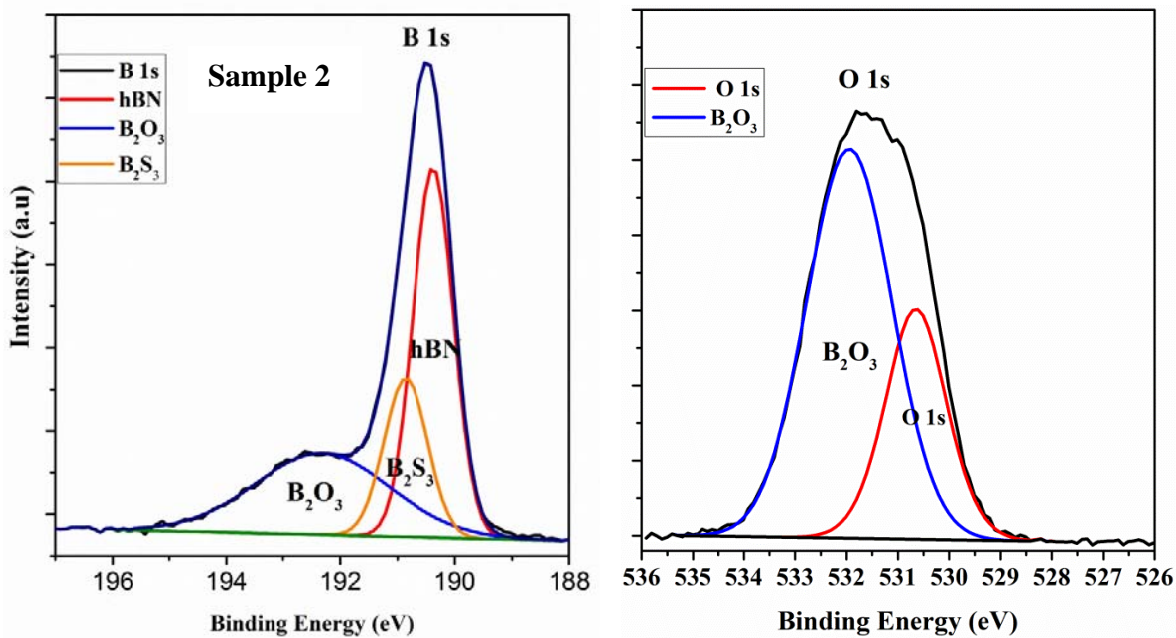


Figure S6: Plot showing the High resolution spectra of B 1s and O 1s collected on a different sample.

As we can see from figure S6, there is a slight non-uniformity with boron-oxygen bonding that was collected on a different sample region. This could be because of the handling of the sample after the exfoliation process i.e., sampling drying environment and transfer of the sample after drying. These conditions might impact the functionalization of the hBN as it can be noticed from the XPS measurements. The individual elemental composition as obtained from the CASA is listed in **table S4**, which corresponds to Figure S4. We can clearly observe that there is a significant increase in the oxidation and addition of species such as Sulfur and Phosphorous in the exfoliated hBN. This indicates that the addition of the components have occurred during the exfoliation process.

Table S5. Elemental composition of hBN as calculated using CASA XPS.

Species	hBN Before exfoliation (%)	hBN After exfoliation (%)
B 1s	33.69	30.6
N 1s	30.39	19.56
O 1s	4.14	29.16
C 1s	31.75	13.95
S 2p	0	2.21
P 2p	0	4.49

References

1. R. V Gorbachev, I. Riaz, R. R. Nair, R. Jalil, L. Britnell, B. D. Belle, E. W. Hill, K. S. Novoselov, K. Watanabe, T. Taniguchi, A. K. Geim, and P. Blake, *Small*, 2011, **7**, 465–8.
2. T. Sainsbury, A. Satti, P. May, Z. Wang, I. McGovern, Y. K. Gun'ko, and J. Coleman, *J. Am. Chem. Soc.*, 2012, **134**, 18758–71.
3. C. Casiraghi, S. Pisana, K. S. Novoselov, a. K. Geim, and a. C. Ferrari, *Appl. Phys. Lett.*, 2007, **91**, 233108.